RESEARCH PAPER

Removal of Azo Dyes Pollutants: Photo Catalyst and Magnetic Investigation of Iron Oxide-Zinc Sulfide Nanocomposites

Rosa Amini [1]**, *Gholamreza Nabiyouni*** [1,*]**, *Saghar Jarollahi*** [2]

[1] *Department of Physics, Faculty of Science, Arak University, Arak, Iran*

[2] *Department of Science, Arak University of Technology, Arak, Iran*

ARTICLE INFO

Article History:
Received 02 August 2020
Accepted 14 November 2020
Published 01 January 2021

Keywords:
Nanocomposite
Nanostructures
Photocatalyst
Precipitation

ABSTRACT

ZnS and iron oxide nanoparticles were first synthesized via precipitation and hydrothermal methods respectively. Fe_3O_4/ZnS nano-composites were then prepared using precipitation method. The prepared products were characterized by X-ray diffraction (XRD), scanning electron microscopy (SEM), and Fourier transform infrared (FT-IR) spectroscopy. Vibrating sample magnetometer (VSM) was used to study the magnetic property of the products. The photo-catalytic behaviour of Fe_3O_4/ZnS nano-composites was evaluated using the degradation of three azo-dyes under ultraviolet light irradiation. The results illustrate super paramagnetic and ferromagnetic behaviour of Fe_3O_4 nanoparticles. The photo catalytic behaviour of Fe_3O_4/ZnS nano-composites was evaluated using the degradation of three various azo dyes under ultraviolet light irradiation. The results show that, the prepared nano-composites are applicable for magnetic and photo catalytic performance.

How to cite this article
Amini R., Nabiyouni Gh., Jarollahi S. Removal of Azo Dyes Pollutants: Photo Catalyst and Magnetic Investigation of Iron Oxide-Zinc Sulfide Nanocomposites. J Nanostruct, 2021; 11(1): 95-104. DOI: 10.22052/JNS.2021.01.011

INTRODUCTION

Synthetic dyes have many applications in industry, for example food, textile, medicine and paper. They might be toxic or carcinogenic for human beings. Discharging of dyes into the ecological systems results in unpleasant effects on human and animal health [1-3]. In the last few decades, wide band gap semiconductor materials have attracted a great attention because of their significant applications in technology and having interesting properties such as size-dependent characteristic [4]. Zinc sulphide (ZnS) is one of the most important semiconductor materials with interesting properties such as a wide direct band gap, (Eg =3.68 eV), high refractive index, high transparency in the visible wavelength region, and large exciton binding energy (40 meV) [5-8]. Because of the important optical properties of ZnS, it has been broadly used as an effective photo-catalyst for the photo-catalytic degradation of organic pollutants, like dyes, p-nitrophenol and halogenated benzene derivatives in wastewater management [5]. Due to fast production of electron–hole pairs by photoexcitation and high negative reduction potentials of the excited electrons, ZnS is considered as an excellent photo-catalyst.

Nevertheless, the easy recombination of e^-/h+ pairs in ZnS reduces the catalytic activity considerably. Additionally, the suspended ZnS photo-catalyst encounters important limitations such as the difficulty in separation, recovery, recycling and high cost in large scale production. Besides, ZnS nanoparticles have a tendency to agglomerate in aqueous solution and prevent the light penetration. In order to overcome to these

* *Corresponding Author Email: g-nabiyouni@araku.ac.ir*

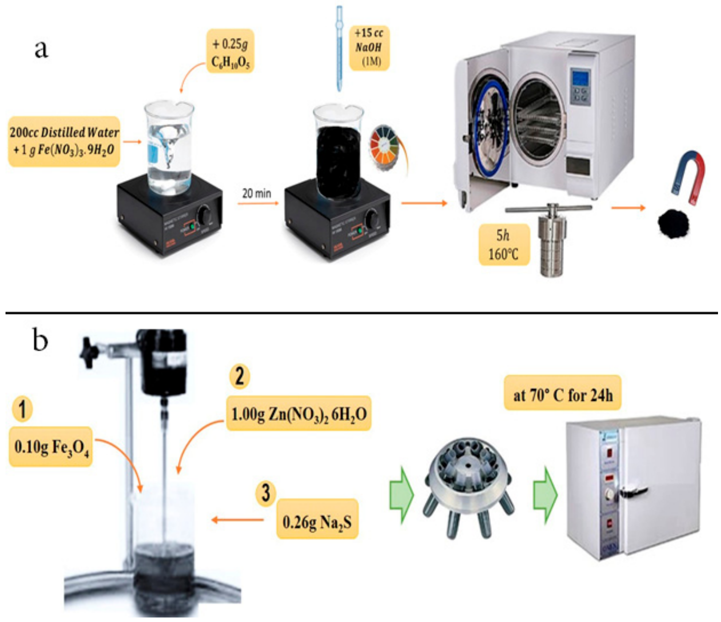

Fig. 1. a) Schematic of Fe_3O_4 nanoparticles preparation b)Schematic of nano-composite preparation

difficulties, ZnS should be coupled with different magnetic semiconducting material. Many researcher groups have used chemical methods for synthesizing the ZnS nanoparticles [9-12]. Since Fe_3O_4 nanoparticles have magnetic property (high coercivity, low Curie temperature and super paramagnetic behaviour), they have been highly studied and exploited. Furthermore, they are non-toxic and biocompatible [13-18].

MATERIALS AND METHODS

Martials

Chemicals: $Fe(NO_3)_3$ $9H_2O$, $Zn(NO_3)_2$ $6H_2O$, NaOH (1M),NH_3, Na_2S, Starch $C_6H_{10}O_5$ and distilled water were used as they were bought from Merck company, without further purification. XRD patterns were recorded by a Philips X-ray diffractometer and using Ni-filtered CuK_α radiation. SEM images were obtained using a LEO instrument model 1455VP. Room temperature magnetic properties were investigated using an vibrating sample magnetometer (VSM) device, (Meghnatis Kavir Kashan Co., Iran) in an applied magnetic field sweeping between ±10000 Oe. Prior to taking SEM images, the samples were coated by a very thin layer of Pt (using a BAL-TEC SCD 005 sputter coater) to make the sample surface conductor and prevent charge accumulation, and obtaining a better contrast. A multiwave ultrasonic generator (Bandeline MS 73), equipped with a converter/transducer and titanium oscillator, operating at 20 kHz with a maximum power output of 150 W was used for the ultrasonic irradiation.

Synthesis of Fe_2O_3 nanoparticles with NaOH deposition factor

First 1.00 g of $Fe(NO_3)_3$ $9H_2O$ was dissolved in 200 ml of distilled water. Then 5ml of NaOH (1M) was slowly added as precipitator. The solution and pH was fixed at 10. The solution was put into an autoclave, and heated at 160°C for 5 horse. The resultant deposit was washed twice with distilled water, collected by centrifuge, and dried at 70° C for 24 hours.

Synthesis of Fe_2O_3 nanoparticles with NH_3 deposition factor

First 1.00 g of $Fe(NO_3)_3$ $9H_2O$ was dissolved in 200 ml of distilled water. Then 15ml of NH_3 was slowly added as precipitator. The rest is similar to which was described above.

Synthesis of Fe_3O_4 nanoparticles

First 1.00 g of $Fe(NO_3)_3$ $9H_2O$ was dissolved in 200 ml of distilled water. 0.25 g of $C_6H_{10}O_5$ was then added to the solution as surfactant, and it was mixed on magnetic stirring for 10 min. Then 15ml of NaOH (1M) was slowly added as precipitator. The pH of solution and was fixed at 10. The above procedure was then repeated. Fig. 1a shows the schematic diagram of experimental setup for preparation of nanoparticles.

Synthesis of ZnS nanoparticles

First 1.00 g of $Zn(NO_3)_2$ $6H_2O$ was dissolved in 200 ml of distilled water and 0.26 g of Na_2S was then added to the solution as surfactant, and it was mixed on a magnetic stirring for 10 minutes. Then 100ml of Na_2S solution was added to solution as precipitator. The solution pH was fixed to 10. The obtained white precipitate was washed twice with distilled water.

Synthesis of ZnS with CH_4N_2S deposition factor

First 1.00 g of $Zn(NO_3)_2$ $6H_2O$ was dissolved in 200 ml of distilled water and 0.26 g of Na_2S was then added to the solution as surfactant, and it was mixed on magnetic stirring for 10 minutes. Then 100ml of Na_2S Solution was added as precipitator. The solution pH was fixed at 10. The obtained white precipitate was washed twice with distilled water.

Synthesis of ZnS with $C_6H_{10}O_5$ deposition factor

First 1.00 g of $Zn(NO_3)_2$ $6H_2O$ was dissolved in 200 ml of distilled water and 0.26 g ofNa_2S was then added to the solution as surfactant, and it was mixed on magnetic stirring for 10 minutes. Then 100ml of Na_2S Solution was added as precipitator. The solution pH was fixed at 10. The obtained white precipitate was washed twice with distilled water.

Synthesis of Fe_3O_4-ZnS nanocomposites

Firstly 0.1 g of synthesized Fe_3O_4 was dispersed in 200 ml of distilled water. It was mixed on mechanical stirrer for 30 minutes. Then 1.00g of $Zn(NO_3)_2$ $6H_2O$ was dispersed for 10 minutes. Then 0.26g of Na_2S added to the solution and was mixed for 20 minutes. The product was then dried in oven at 70° C for 24 hours. Fig. 1b shows the schematic diagram of experimental setup for preparation of nanoparticles.

Photo-catalytic degradation process

10 ml of the dye solution (20 ppm) was used as a model pollutant to determine the photo-catalytic activity. 0.1 g catalyst was applied for degradation of 10 ml solution. The solution was mixed by a magnetic stirrer for 1 hour in darkness to determine the adsorption of the dye by catalyst and better availability of the surface. The solution was irradiated by a 100 Watts UV lamp which was placed in a quartz pipe in the middle of reactor. It was turned on after 1 hour stirring of the solution and sampling (about 10 ml) was done every 15 min. The samples were filtered, centrifuged and their concentration was determined by UV-Visible spectrometry.

RESULTS AND DISCUSSION

Fig. 2a shows the XRD patterns of Fe_2O_3 nanoparticles. The pattern shows a rhombohedral structure, accordance with JCPDS card No. 0664-33 for hematite iron oxide.

Fig. 2b shows the XRD patterns of Fe_3O_4 nanoparticles. The pattern shows a cubic structure, accordance with JCPDS card No. 01-111, with Fd-3m space group for iron oxide.

Fig. 2c shows the XRD patterns of ZnS nanoparticles. The pattern shows a cubic structure, which is accordant to JCPDS card No. 80-200, with F-43m space group for Zinc sulphide.

Fig. 2d shows the XRD pattern the Zinc sulphide -iron oxide composite. The average crystalline size for iron oxide, Zinc sulphide and nanocomposites were found to be about 30 and 50 nm respectively. SEM analyses show (in three different magnifications) the formation of essentially spherical Zinc sulphide nanoparticles (with CH_4N_2S as deposition factor) and the agglomeration of particles can be observed (Fig. 3a). The image also indicate that the nanoparticles with average diameter size of less than 55 nm were prepared. Fig. 3b exhibits SEM image of Zinc sulphide nanoparticle (with $C_6H_{10}O_5$ deposition factor) with average size of less than 55 nm. Fig. 3c exhibits SEM image of Zinc sulphide (with a Na_2S) nanoparticle with average size less of than 65 nm. Fig. 3d exhibits SEM images of iron oxide nanoparticles (with NH_3 as deposition factor) that synthesized by hydrothermal method. The results approve formation of nanoparticles with average size of less than 30 nm. As can be seen, almost spherical particle morphologies have been created. Fig. 4a exhibits SEM image of iron oxide nanoparticle (with NaOH as deposition factor) which prepared by hydrothermal method. The results approve formation of nanoparticle with average size less than 50 nm. Fig. 4b exhibits SEM image of iron oxide nanoparticle (with $C_6H_{10}O_5$ as deposition factor) that achieved by hydrothermal method. The results approve formation of nanoparticle with average size less than 45 nm.

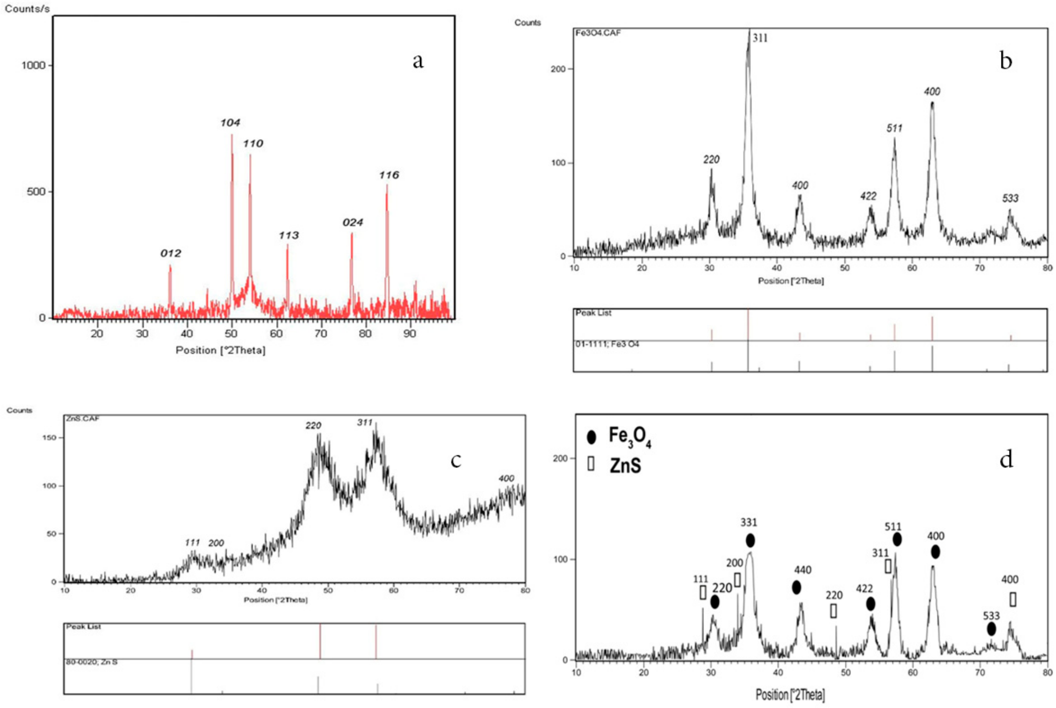

Fig. 2. XRD patterns of a) Fe_2O_3 nanoparticles b) Fe_3O_4 nanoparticles c) ZnS nanoparticles d) iron oxide-zinc sulphide nano-composite

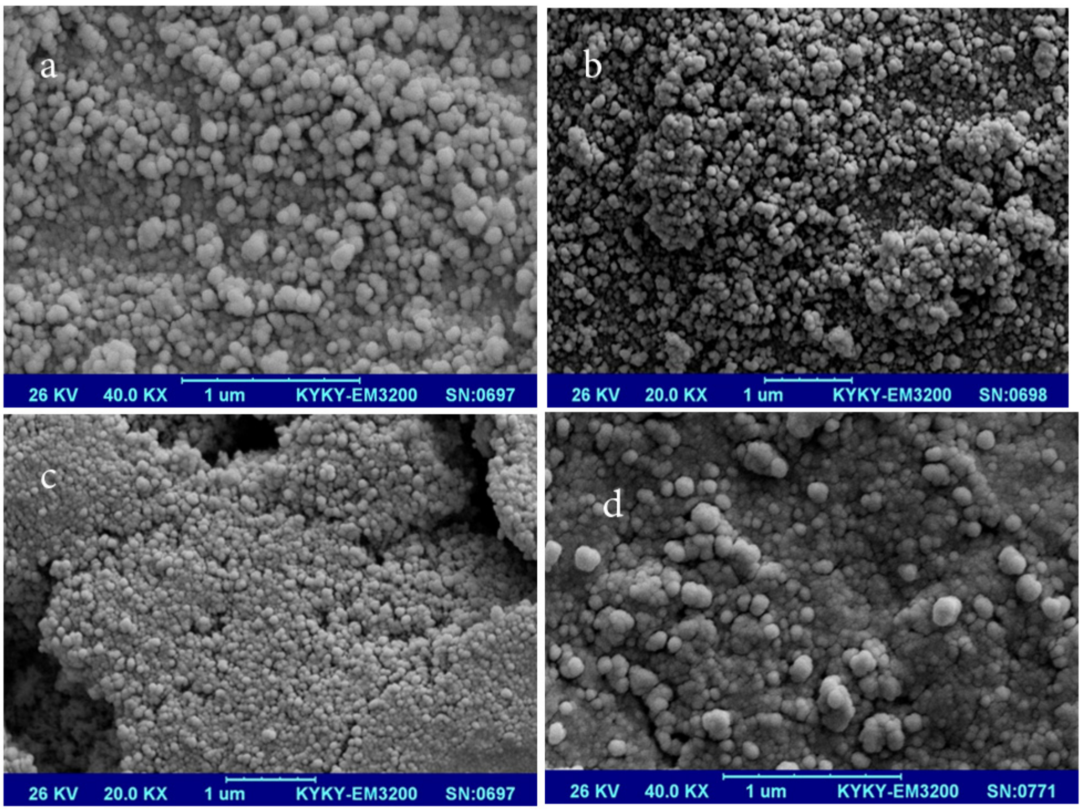

Fig. 3. SEM images of a) zinc sulphide with CH_4N_2S deposition factor b) zinc sulphide with $C_6H_{10}O_5$ deposition factor c) zinc soulphide with Na_2S deposition factor d) Fe_2O_3 with NH_3 deposition factor

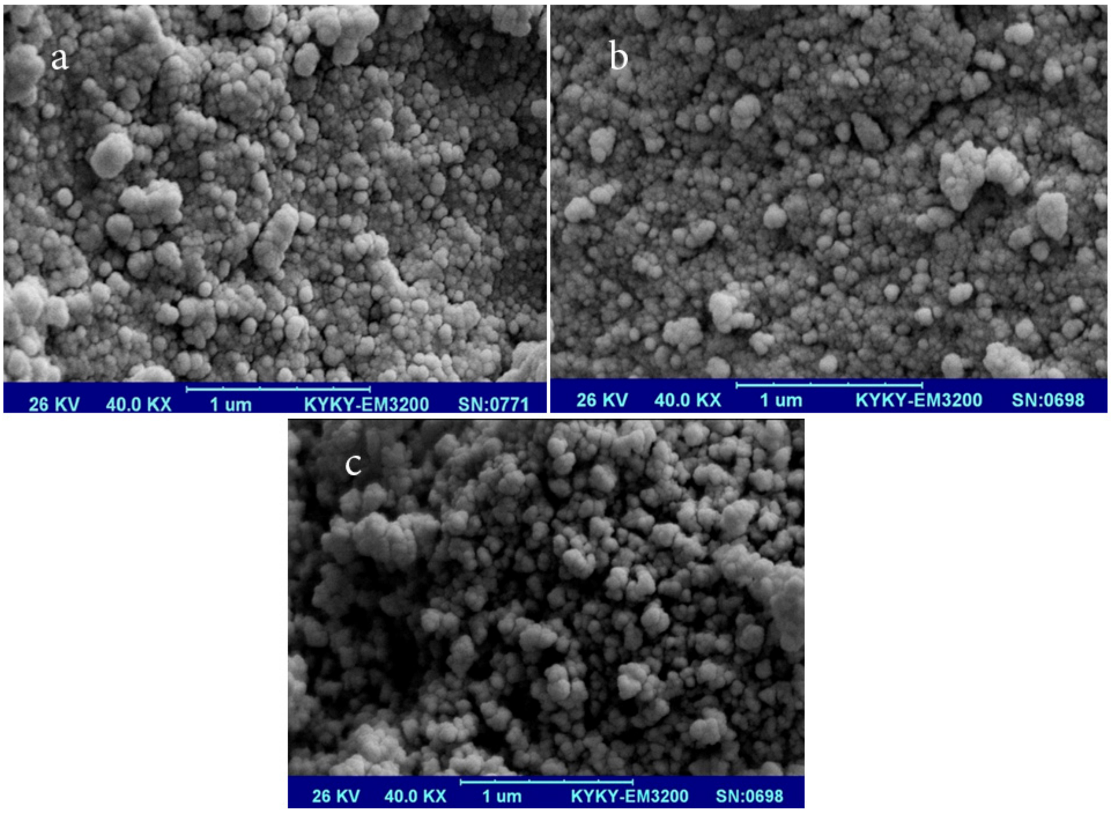

Fig. 4. SEM images of a) Fe_2O_3 with NaOH deposition factor b) Fe_3O_4 with $C_6H_{10}O_5$ deposition factor c) iron oxide-zinc sulphide nano-composite

The nano-composites which their SEM image is presented in Fig. 4c, was synthesized with a iron oxide to zinc sulphide ratio of 1:1. Mono-dispersed product was prepared, that approve by addition of ZnS shell on the iron oxide core. Still the nanostructures with average size of less than 100 nm were synthesized.

Room temperature magnetic properties of samples were studied using VSM instrument. Hysteresis loop for iron oxide nanoparticles is shown in Fig. 5a, which indicates iron oxide nanoparticles exhibit super paramagnetic behaviour with a coercivity of 13.8 Oe and a saturation magnetization of 24.5 emu/g. Fig. 5b shows magnetization loop of iron oxide-zinc sulphide with a coercivity of about 26.6 Oe and a saturation magnetization of 2.3 emu/g. Magnetization has dropped slightly due to the presence of zinc sulphide in the nano-composites, but it can still be absorbed by a small magnet, which promise that it is suitable and has a useful property for wastewater treatment.

Fig. 6a shows the FT-IR spectrum of the as-prepared iron oxide nanoparticles. The absorption bands at 472 and 576 cm^{-1} are assigned to the Fe-O stretching mode. The spectrum exhibits a broad absorption peak near 3417 cm^{-1}, corresponding to the stretching mode of O-H group of hydroxyl groups. Fig. 6b shows the FT-IR spectrum of the as-prepared zinc sulphide nanoparticles. The absorption bond at 492 and 617 cm^{-1} is assigned to the S-O (metal-oxygen bonds) stretching mode. The spectrum exhibits a broad absorption peak around 3377 cm^{-1}, corresponding to the stretching mode of O-H group of hydroxyl group. FT-IR spectrum of the iron oxide-zinc sulphide nano-composite is shown in Fig. 6c. Absorptions bands at 664, 577 and 531 cm^{-1} which approve the presence of magnetic nanoparticles are clearly observed. A weak bond near 3417 cm^{-1} is also observed which is assigned to H–O–H bending vibration mode due to the adsorption of moisture on the nanoparticles surface. There are no other significant peaks related to precursors and other impurities.

The photo-catalytic activity of iron oxide-

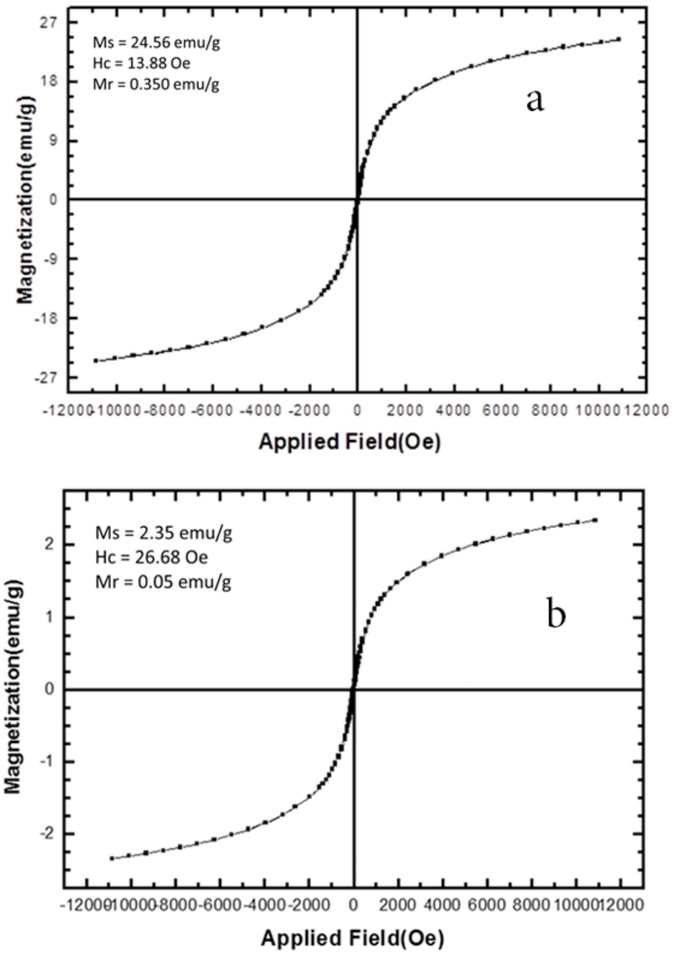

Fig. 5. Hysteresis loops of a) iron oxide nanoparticles b) iron oxide-zinc sulphide nano-composite

zinc sulphide nano-composite and zinc sulphide nanoparticle was evaluated by monitoring the degradation of three azo dyes in an aqueous solution, under irradiation of UV light. In this work, for more efficiently removal and in the shorter time of degradation of azo dyes, ultraviolet light is used. Figs.7-9 show the UV-visible absorption spectra revealing that, UV light irradiation induced photocatalytic degradation of azo dyes by using the as-synthesized iron oxide-zinc sulphide nano-composite and zinc sulphide nanoparticle. In photocatalytic activity, firstly, with the appropriate wavelength of light, electrons and holes are generated. The photo-generated holes react with adsorbed H_2O on the catalyst surface to form hydroxyl radicals (H_2O + h+V_B •OH), the radicals which are known to be the most powerful oxidizing species for organic pollutants. In other reaction, the excited electrons in the conduction band move to the surface and reduce of oxygen molecules adsorbed on the nanoparticles' surface, producing of superoxide anion radicals (O^{2+} e– CB •O^{2-}). Organic dyes decompose to water, carbon dioxide and other less toxic or nontoxic residuals by superoxide anion and hydroxyl radicals. The higher photocatalytic activity of iron oxide-zinc sulphide nano-composite is attributed to the efficient charge separation and increased production of superoxide anion and hydroxyl radicals. Schematics of the photocatalytic properties mechanism of iron oxide-zinc sulphide nano-composite under UV is shown in Figs. 10 and 11. Fig. 12 shows the degradation of three azo dyes after 30 min (for acid black), 40 min (for acid brown) and 60 min (for methylene blue) exposure of UV radiation in the presence of iron oxide-zinc sulphide nano-composite.

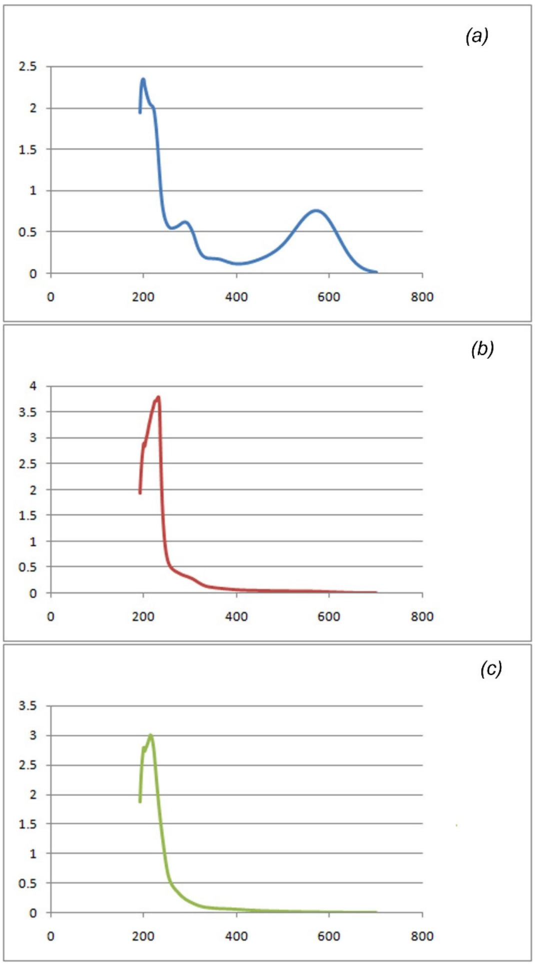

Fig. 6. FT-IR spectrum of a) iron oxide nanoparticles b) zinc sulphide nanoparticles c) iron oxide-zinc sulphide nano-composite

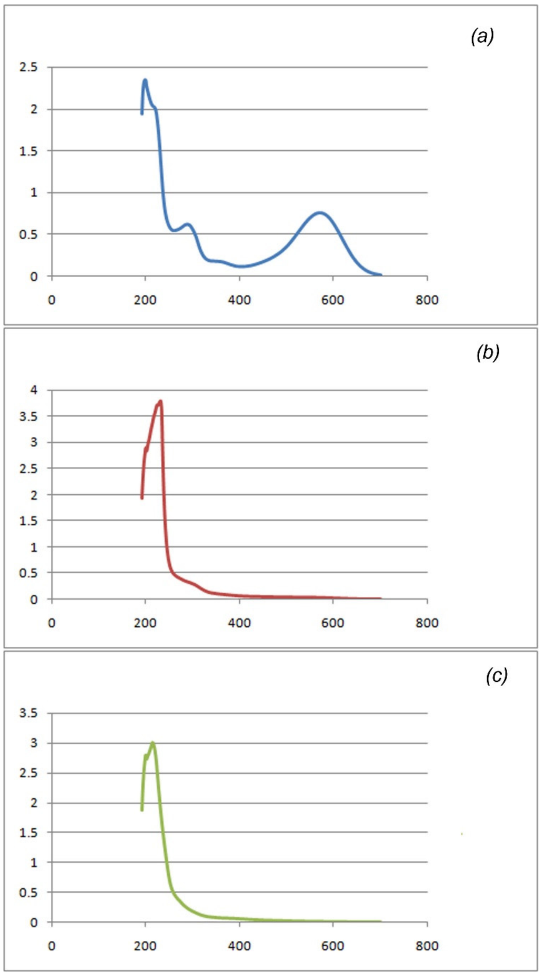

Fig. 7. UV–Vis spectra of degradation of acid black a) 0 min, b) 30 min in the presence of ZnS nanoparticles, c) 30 min in the presence of nano composite

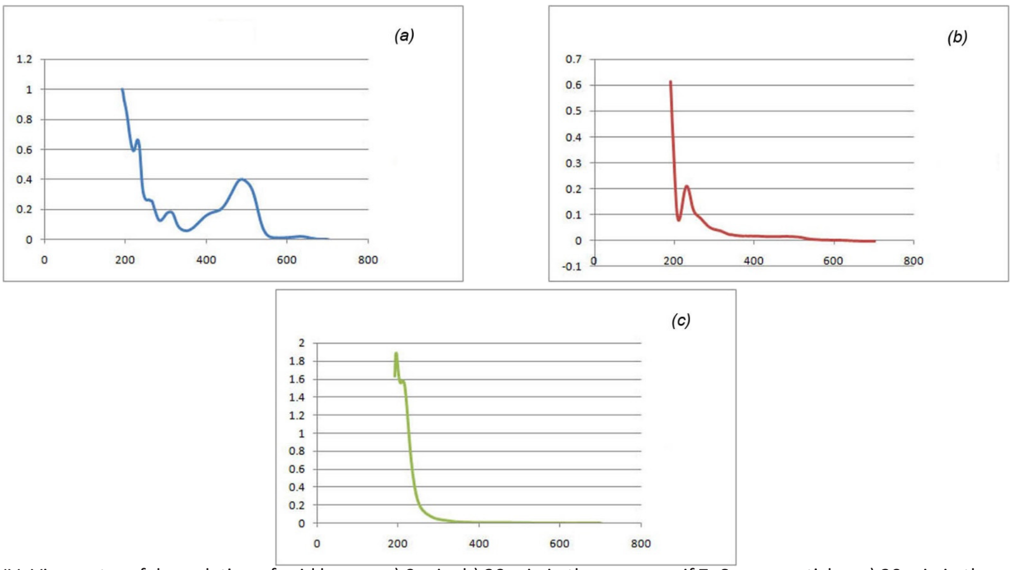

Fig. 8. UV–Vis spectra of degradation of acid brown a) 0 min, b) 30 min in the presence if ZnS nanoparticles, c) 30 min in the presence of nano composite

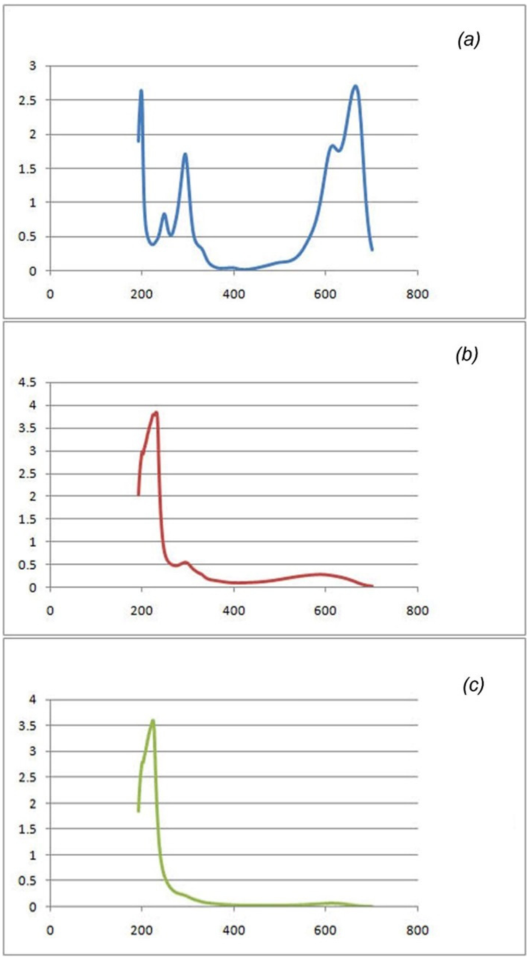

Fig. 9. UV–Vis spectra of degradation of methylene blue a) 0 min, b) 30 min in the presence of ZnS nanoparticles, c) 30 min in the presence of nano composite

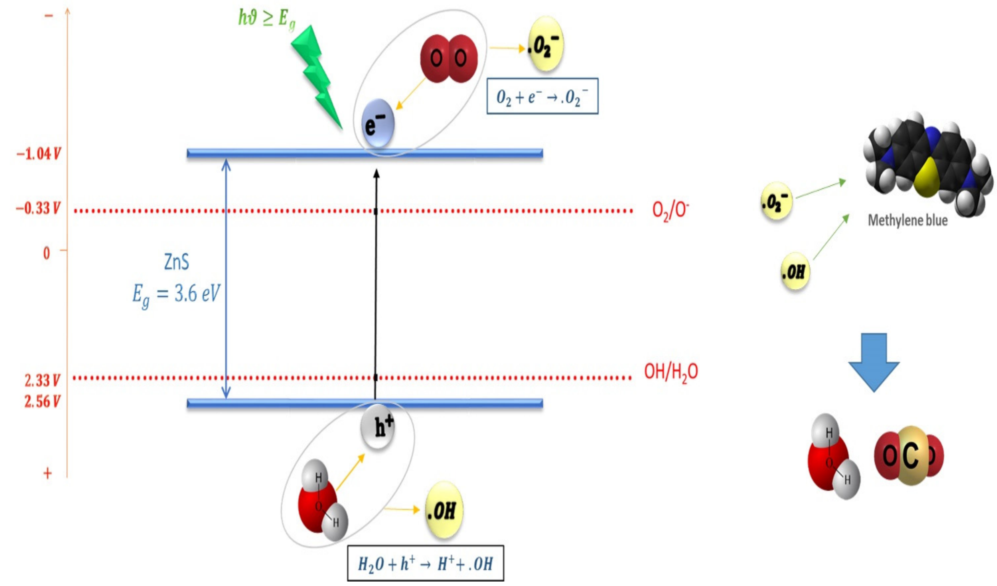

Fig. 10. Schematic of the mechanism of photocatalytic properties of iron oxide/zinc soulphide nano-composite under UV light

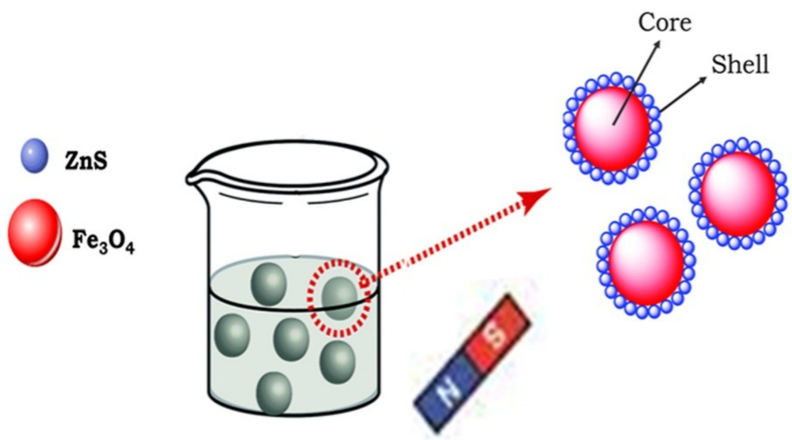

Fig. 11. Schematic of core-shell formation

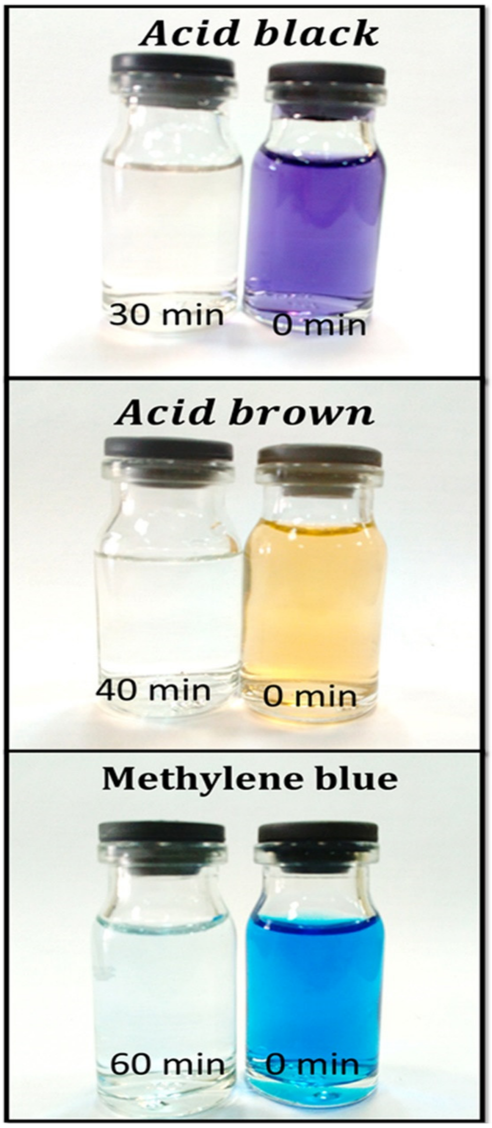

Fig. 12. Photocatalytic activity of iron oxide-zinc sulphide nano-composite

CONCLUSIONS

In conclusion, synthesis, characterization, and photocatalytic activity of Iron Oxide-Zinc sulphide nano- composite was reported. VSM measurements confirmed that nanoparticles and nano-composites exhibit paramagnetic behaviour. A naturally occurring and non-toxic magnetism core for humans was prepared in a simple hydrothermal method without the need of chemical and expensive precursors. It is concluded that the transfer of the charge carriers and separation them, leads to high production of free radicals. The significant reduction in the charge carrier recombination, account for the enhanced efficiency of photocatalytic decomposition of azo dyes by UV light.

CONFLICT OF INTEREST

The authors declare that there is no conflict of interests regarding the publication of this manuscript.

REFERENCES

1. Safardoust-Hojaghan H, Salavati-Niasari M. Degradation of methylene blue as a pollutant with N-doped graphene quantum dot/titanium dioxide nanocomposite. Journal of Cleaner Production. 2017;148:31-6.
2. Farhadi S, Siadatnasab F, Khataee A. Ultrasound-assisted degradation of organic dyes over magnetic $CoFe_2O_4$@ZnS core-shell nanocomposite. Ultrasonics Sonochemistry. 2017;37:298-309.
3. Hu W, Yu X, Hu Q, Kong J, Li L, Zhang X. Methyl Orange removal by a novel PEI-AuNPs-hemin nanocomposite. Journal of Environmental Sciences. 2017;53:278-83.
4. Petronella F, Truppi A, Ingrosso C, Placido T, Striccoli M, Curri ML, et al. Nanocomposite materials for photocatalytic degradation of pollutants. Catalysis Today. 2017;281:85-100.
5. Qutub N, Pirzada BM, Umar K, Mehraj O, Muneer M, Sabir S. Synthesis, characterization and visible-light driven photocatalysis by differently structured CdS/ZnS sandwich and core–shell nanocomposites. Physica E: Low-dimensional Systems and Nanostructures. 2015;74: 74-86.
6. Raleaooa PV, Roodt A, Mhlongo GG, Motaung DE, Kroon RE, Ntwaeaborwa OM. Luminescent, magnetic and optical properties of ZnO-ZnS nanocomposites. Physica B: Condensed Matter. 2017;507:13-20.
7. Hart JN, Cutini M, Allan NL. Band Gap Modification of ZnO and ZnS through Solid Solution Formation for Applications in Photocatalysis. Energy Procedia. 2014;60:32-6.
8. Moore D, Wang ZL. Growth of anisotropic one-dimensional ZnS nanostructures. Journal of Materials Chemistry. 2006;16(40):3898.
9. Stefan M, Leostean C, Pana O, Soran ML, Suciu RC, Gautron E, et al. Synthesis and characterization of Fe_3O_4@ZnS and Fe_3O_4@Au@ZnS core–shell nanoparticles. Applied Surface Science. 2014;288:180-92.
10. Wei Y, Han B, Hu X, Lin Y, Wang X, Deng X. Synthesis of Fe_3O_4 Nanoparticles and their Magnetic Properties. Procedia Engineering. 2012;27:632-7.
11. Joulaei M, Hedayati K, Ghanbari D. Investigation of magnetic, mechanical and flame retardant properties of polymeric nanocomposites: Green synthesis of $MgFe_2O_4$ by lime and orange extracts. Composites Part B: Engineering. 2019;176:107345.
12. Ahmadian-Fard-Fini S, Salavati-Niasari M, Ghanbari D. Hydrothermal green synthesis of magnetic Fe_3O_4-carbon dots by lemon and grape fruit extracts and as a photoluminescence sensor for detecting of E. coli bacteria. Spectrochimica Acta Part A: Molecular and Biomolecular Spectroscopy. 2018;203:481-93.
13. Eskandari N, Nabiyouni G, Masoumi S, Ghanbari D. Preparation of a new magnetic and photo-catalyst $CoFe_2O_4$–$SrTiO_3$ perovskite nanocomposite for photo-degradation of toxic dyes under short time visible irradiation. Composites Part B: Engineering. 2019;176:107343.
14. Saffarzadeh S, Nabiyouni G, Ghanbari D. Preparation of $Ni(OH)_2$, NiO and $NiFe_2O_4$ nanoparticles: magnetic and photo-catalyst $NiFe_2O_4$–NiO nanocomposites. Journal of Materials Science: Materials in Electronics. 2016;27(12):13338-50.
15. Kiani A, Nabiyouni G, Masoumi S, Ghanbari D. A novel magnetic $MgFe_2O_4$–$MgTiO_3$ perovskite nanocomposite: Rapid photo-degradation of toxic dyes under visible irradiation. Composites Part B: Engineering. 2019;175:107080.
16. Moradi B, Nabiyouni G, Ghanbari D. Rapid photo-degradation of toxic dye pollutants: green synthesis of mono-disperse Fe_3O_4–CeO_2 nanocomposites in the presence of lemon extract. Journal of Materials Science: Materials in Electronics. 2018;29(13):11065-80.
17. Etminan M, Nabiyouni G, Ghanbari D. Preparation of tin ferrite–tin oxide by hydrothermal, precipitation and auto-combustion: photo-catalyst and magnetic nanocomposites for degradation of toxic azo-dyes. Journal of Materials Science: Materials in Electronics. 2017;29(3):1766-76.
18. Naghikhani R, Nabiyouni G, Ghanbari D. Simple and green synthesis of $CuFe_2O_4$–CuO nanocomposite using some natural extracts: photo-degradation and magnetic study of nanoparticles. Journal of Materials Science: Materials in Electronics. 2017;29(6):4689-703.